Arch. Mech., 37, 4–5, pp. 535—548, Warszawa 1985

Local destruction of granular media caused by crushing a single grain

J. A. SUPEL (WARSZAWA)

THE PARTICLE crushing effect and its influence on the microscopic deformation mechanism is examined. The results of a number of experiments on biaxial deformation of assemblies of discs are analysed focusing attension on the evolution of the microstructure around a crushed grain. Two kinds of the equipment are employed: horizontal table with discs made of soft polyuretane and vertical frame with discs of high stiffness plexiglass. As a result of crushing of a single grain, located at the center of the sample, the large local displacements of grains are observed. The average strain rate tensor and fabric tensor are calculated. The physical tests are reproduced numerically, using the distinct element method, by repeating the experiment with the same geometry but different values of stiffness at contact points between grains.

Badany jest wpływ kruszenia się pojedynczego ziarna na mechanizm deformacji. Przedstawiono wyniki eksperymentów polegających na dwuosiowym ściskaniu zbioru płaskich krążków, skupiając uwagę na zmianach struktury wokół ziarna. Używano dwu rodzajów stanowisk badawczych: poziomo ustawiony stół z krążkami wykonanymi z miękkiego poliuretanu oraz pionowa rama ze sztywnymi krążkami. Jako rezultat kruszenia jednego ziarna, znajdującego się w środkowej części próbki, obserwowano znaczne przemieszczenie ziaren. Obliczono średni tensor prędkości odkształcenia i tensor tekstury. Doświadczenia fizyczne odtworzono numerycznie, używając metody elementów kontaktowych, przez powtórzenie geometrii krążków lecz dla różnych sztywności w punktach kontaktu między krążkami.

Исследуется влияние дробления единичного зерна на механизм деформации. Представлены результаты экспериментов, заключающихся в двуосевом сжатии совокупности плоских дисков, сосредоточивая внимание на изменениях структуры вокруг дробленного зерна. Использованы два типа исследовательских установок: горизонтально расположенный стол с дисками, изготовленными из мягкого полиуретана, а также вертикальная рама с жесткими дисками. Как результат дробления единичного зерна, находящегося в средней части образца, наблюдалось значительное перемещение зерен. Вычислены средний тензор скорости деформации и тензор текстуры. Физические эксперименты воспроизведены численно, используя методы контактных элементов путем повторения геометрии дисков, но для разных жесткостей в точках контакта между дисками.

1. Introduction

IT IS COMMONLY accepted that the mechanical behaviour of granular media is strongly affected by their microstructures, namely the granular fabric. The changes of the fabric have an effect on the hardening or softening of the granular materials in a given deformation process [10, 19]. It is usually assumed that the global plastic deformation of cohesionless granular materials consists of the local frictional slidings between grains and particle rolling, [14, 15, 20]. However, sliding and rolling of grains are not the only cause of changes of the microstructure. It has been commented on in the literature that the particle-crushing effect does take place during the flow of the cohesionless granular material, and a part of the grains breaks at even relatively low stress level, see for example [5, 9, 13, 22]. Up to 30% of grains are crushed (eg. are divided into two or more parts)

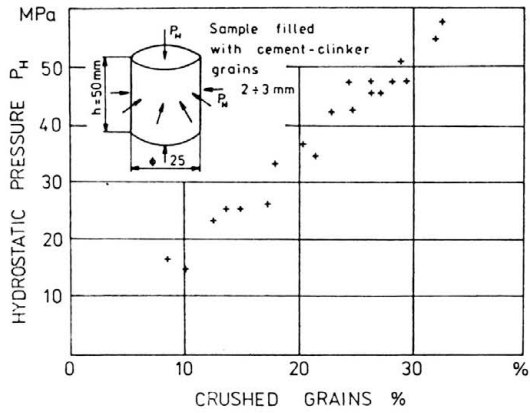

FIG. 1. Particle crushing effect in hydrostatic compression of grains of cement clinker.

in triaxial hydrostatic compression [22]; see Fig. 1. This crushing effect in the shear processes is more strongly visible [8, 12].

The crushing phenomenon of particles is not included in the known macroscopic constitutive relations of granular media. The main purpose of the present work is to examine the extent of the particle crushing effect and its influence on the microscopic deformation mechanism. However, the interpretation of the crushing phenomenon on real granular media, like sand, gravel or rockfill, is difficult because the local processes inside the sample cannot be observed. Hence a special material model must be used.

To this end, the results of a number of experiments on biaxial deformations of assemblies of photoelastic discs are analysed, focussing attention on the evolution of the microstructure around a crushed grain.

An attempt was made to duplicate numerically the physical tests. The numerical model of the granular material, with the particle-crushing effect added, was used. It was possible to investigate the effect of crushing on the behaviour of the assembly by repeating the experiment with the same geometry but different values of stiffness at the contact of grains.

2. Experiment

Research was led in two different ways. Figure 2 presents the stand which was used to investigate on the horizontal table ([1]). The test area, about half a square meter, was filled with approximately 1500 discs made of a 12 mm thick plate of polyurethane rubber, a sensitive photoelastic material. Seven various diameters of discs were used, ranging from 10 to 60 mm.

The scheme of the testing apparatus is shown in Fig. 3. The sample was formed within the loading frame of initial dimensions of about 650×750 mm. Each sample consisted of equal numbers of particles of seven sizes. Particles were stocked by hand randomly. The assembly of discs was loaded by means of two pairs of rigid beams which formed

([1]) These experiments were performed in Laboratorio de Rocamientes, Instituto de Ingenieria, Universidad Nacional Autonoma de Mexico.

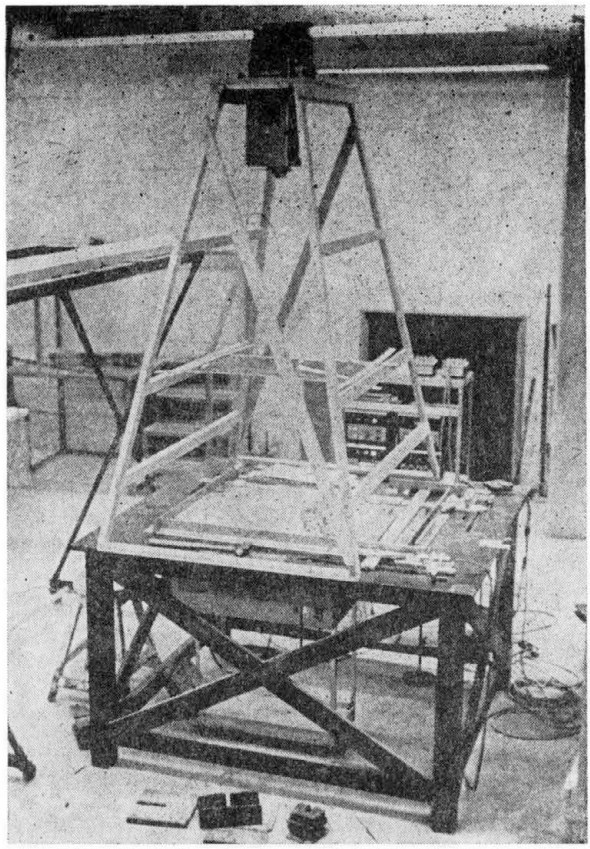

FIG. 2. Whole view of biaxial frame with 1500 discs (Rockfill Laboratory, UNAM, Mexico).

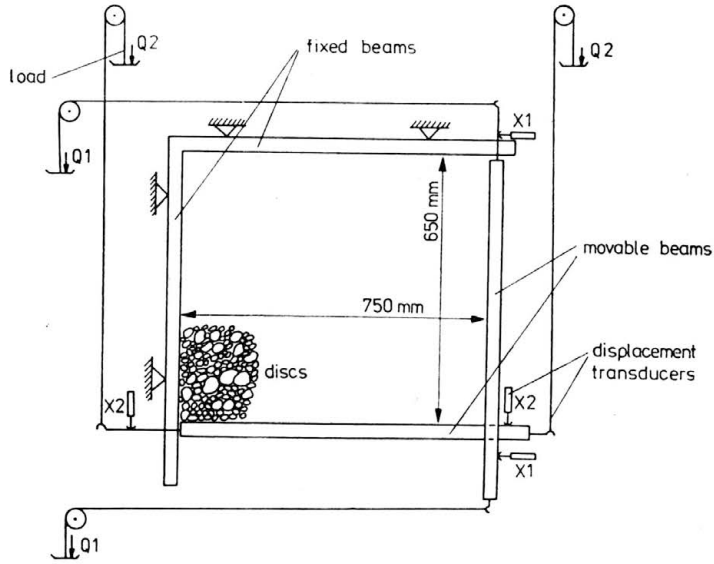

FIG. 3. Sketch of biaxial testing apparatus for 1500 discs.

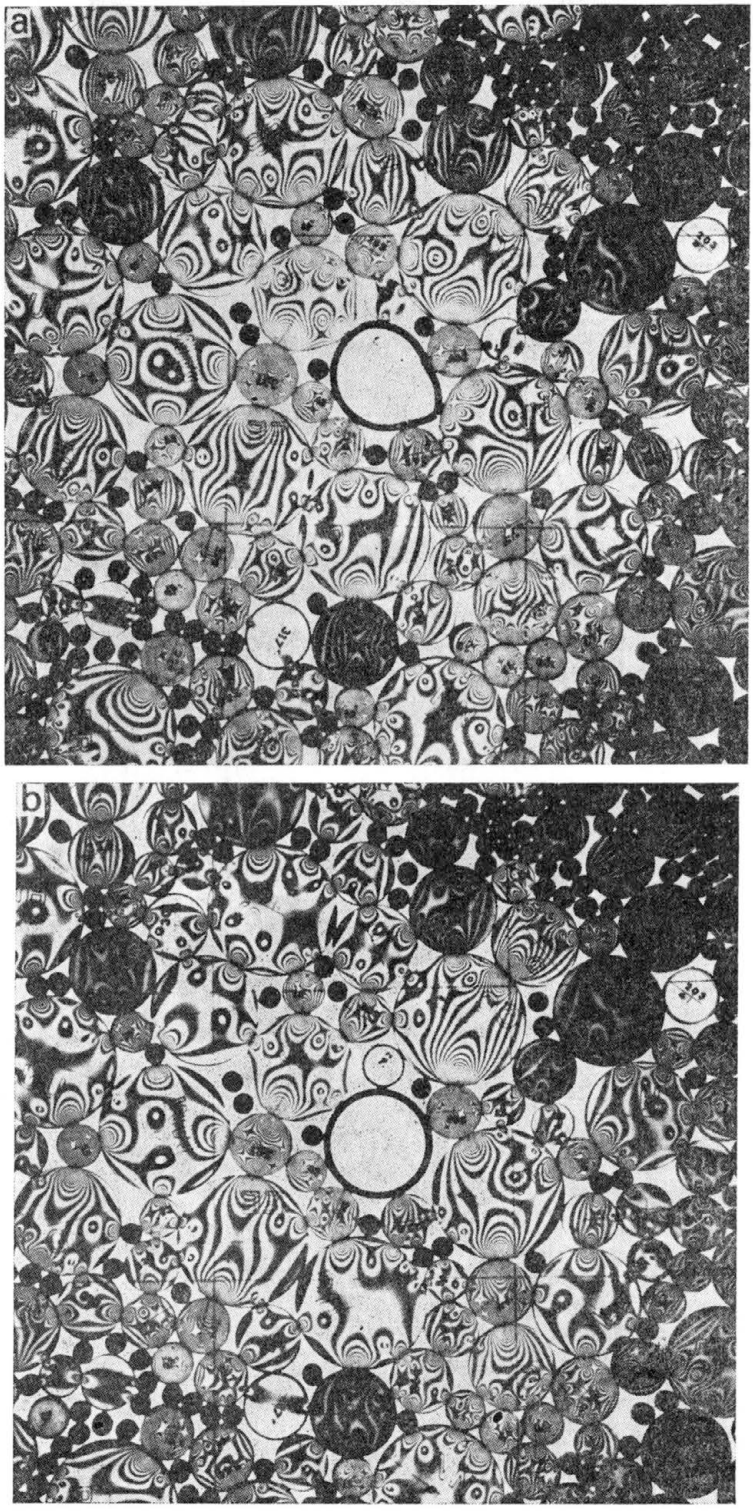

FIG. 4. The central part of sample, around crushed ring, a) after crushing, b) before crushing.

the boundaries. Two of these beams were free to move and rotate. The moving beams were subjected to forces by change of weights. The displacements of ends of each beam were measured by four LVDT's. At the central part of the sample the brittle ring was placed; see Fig. 4.

As a result of crushing of a single grain, located at the center of the sample, large local displacements of grains apeared. Photoelastic photographs were taken at an appropriate stage during the course of deformation, which enabled to determine the relative displacement of each grain.

Another testing apparatus ([2]) is shown in Fig. 5. It consists of an overall frame within which a biaxial loading frame is mounted. The sample was formed within the loading frame of initial dimensions about 220 mm in height and 210 mm in width. Each sample consisted of equal numbers of discs. The discs had nine various diameters, ranging from

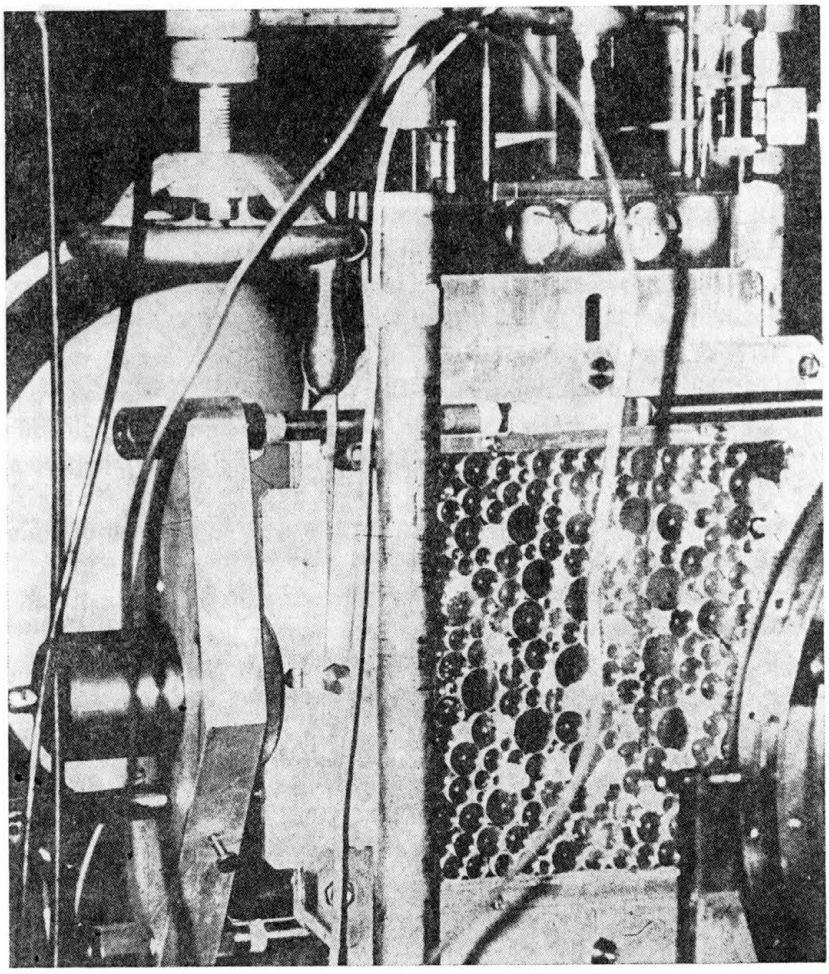

FIG. 5. Test apparatus (Institute of Fundamental Technological Research, Warsaw).

([2]) These experiments were performed in the Institute of Fundamental Technological Research, Warsaw

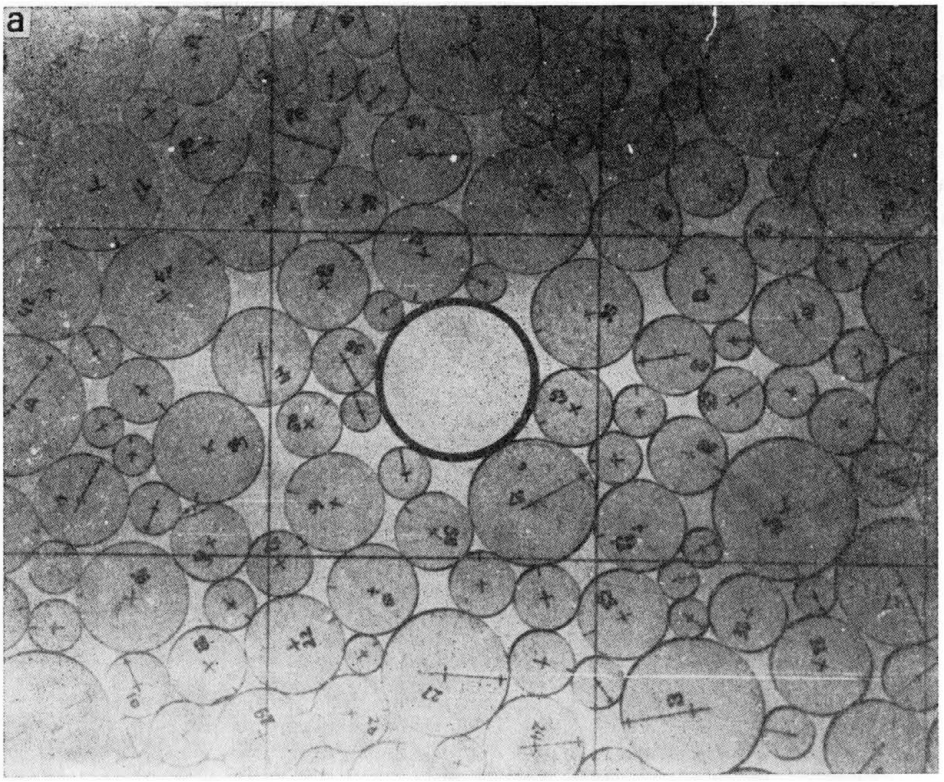

FIG. 6a. Sample with hard plexiglass discs.

6 to 25 mm, the common thickness was 5 mm, and they were made of high stiffness plexiglass. The sample was confined laterally by constant forces (1–4 kN depending on the test). The horizontal load was measured by a load transducer and the horizontal and vertical displacements by LVDT's. Figure 6 shows a typical photograph of grain crushing in the central part of a sample.

3. Fabric and strain description

The above experiments yield discrete quantities that are useful in studying the material behaviour on a microscale, but cannot be transferred directly to a continuum model. Averaging procedures are necessary to make the step from the microscale to a continuum. The definition and calculation of most average quantities, like density or the number of contacts, are reported elsewhere; see [23]. The average number of contacts and its distribution yield first-order information for the description of the granular materials. Since it is a scalar, it does not describe the spatial orientations of contacts. For the purpose of more information we must look for other parameters.

3.1. Distribution of contact normals; fabric tensor

The term "fabric" is used in this paper to identify the arrangement of the particles. Figure 7a shows an assembly of discs, statistically distributed. Without loss of general-

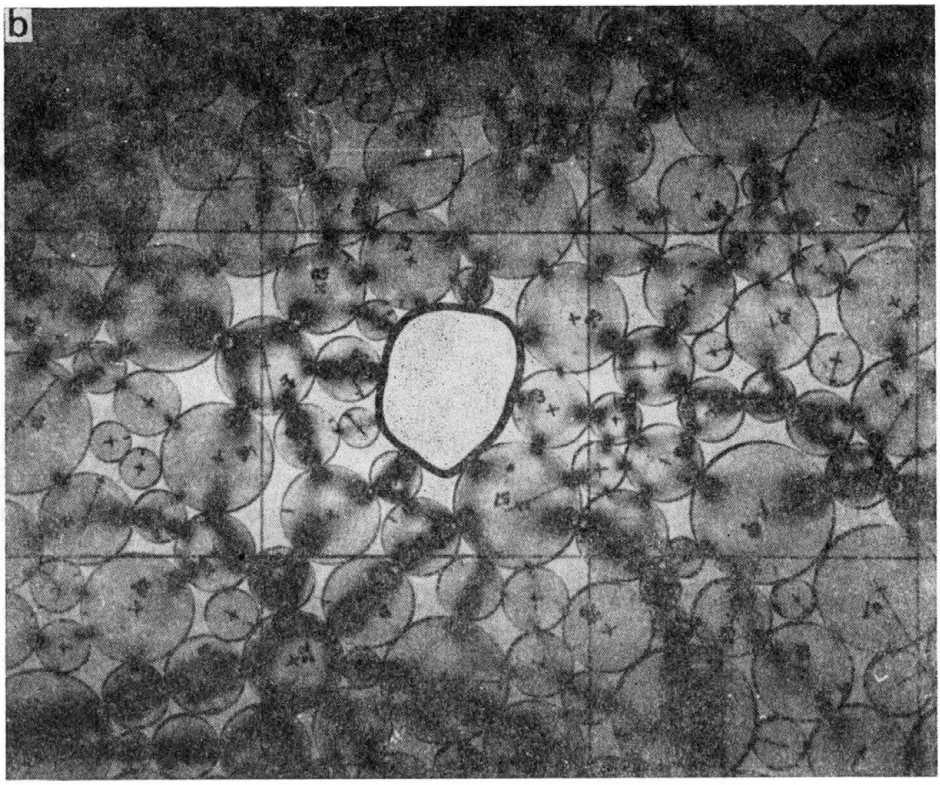

FIG. 6b. Sample with hard plexiglass discs.

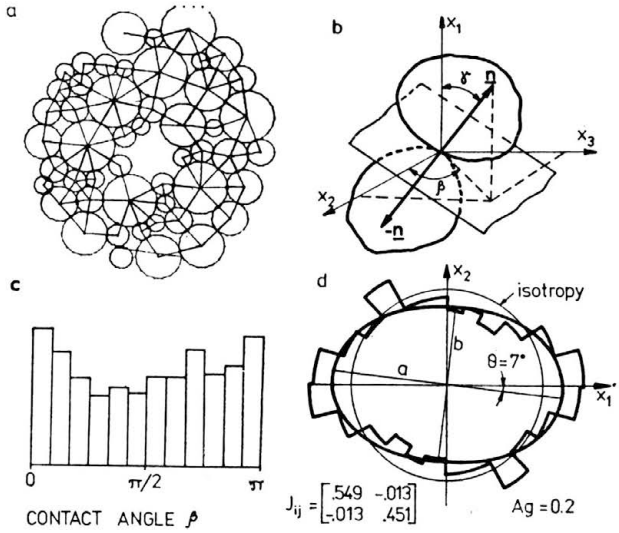

FIG. 7. Fabric in deformed granular materials: a) connection map of statistically distributed grains, b) contact with normal vectors, c) frequency distribution of contact angle, d) ellipse of geometric anisotropy.

ity, the assembly of discs (or generally spheres) can be replaced by an assembly of points and lines. There are points marking the centers of particles, and lines connecting the centers of adjacent particles which are in contact. We shall call this line "branch". A description of these branches gives more information about the structure of grains. Since grains are discs (or spheres), the branch is equivalent to a normal vector at contact point. The normal vectors may be identified by angles γ and β with respect to a fixed rectangular Cartesian coordinate system; Fig. 7b. The probability density function $\mathbf{E}(n)$, which was introduced by HORNE [6,7] and ODA [16], describes the angular distribution of contact unit normals $\mathbf{n}$. The function $\mathbf{E}(n)$ satisfies:

$$\iint_{\Omega} \mathbf{E}(n)d\Omega = 1, \quad \mathbf{E}(n) = \mathbf{E}(-n). \tag{3.1}$$

For example, for the discs assembly shown in Fig. 7a we can measure the angle β at all contacts between grains and prepare the frequency distribution of β as Fig. 7c shows. As it was discussed in [17], experimental results suggest that the density function $\mathbf{E}(n)$ may be represented with good accuracy by an ellipsoid. Basing on this fact ODA, NEMAT-NASSER, MEHRABADI [18] have defined the "fabric tensor"

$$F_{ij} = N\hat{l}\iint_{\Omega} n_i n_j \mathbf{E}(n)d\Omega = N\hat{l}\langle n_i n_j\rangle, \tag{3.2}$$

where the N — number of contacts, $\hat{l}$ — mean branch length and the term $\langle n_i n_j\rangle$ means

$$\langle n_i n_j\rangle \equiv \frac{1}{N}\sum_{\alpha=1}^{N} n_i^{\alpha} n_j^{\alpha}, \tag{3.3}$$

where n_i, n_j are components of the unit normal vector at contact. That fabric may be represented by a second-order tensor as it has been previously pointed out by SATAKE [21] in the form

$$\bar{J}_{ij} = \langle n_i n_j\rangle. \tag{3.4}$$

In other words we can say that the fabric tensor describes geometrical anisotropy. Geometrical anisotropy was studied by BIAREZ and WIENDIECK [1], as a dip of the contact planes for two-dimensional granular media. The results of measurements are well approximated by an ellipse whose semi-axes a, b define the degree of geometric anisotropy A_g according to the relation

$$A_g = \frac{a-b}{a+b}. \tag{3.5}$$

In the case of geometric isotropy $a = b$ and $A_g = 0$; see Fig. 7d. It is easy to see that the geometrical anisotropy can be calculated from Satake's fabric tensor; for a two-dimensional case the fabric tensor components are expressed by

$$\begin{aligned} J_{ii} &= 1, \\ J_{11} - J_{22} &= 1/2 A_g \cos 2\theta, \\ J_{12} = J_{21} &= 1/4 A_g \sin 2\theta, \end{aligned} \tag{3.6}$$

where θ is an angle to the predominant direction of the normals to the contact planes. This designation of the fabric tensor and anisotropy is also used in this paper.

3.2. Average strain rate tensor

In the present experiment the rotations of the discs were not measured and for averaging of the displacement gradient tensor the technique used by DRESHER and DE JOSSELYN DE JONG [4] was chosen. The average displacement gradient tensor α_{ij}, calculated in domain V, may be written as

$$\bar{\alpha}_{ij} = u_{i,j} = \frac{1}{V}\int_V u_{j,i}dV, \tag{3.7}$$

where u_j, $j = 1, 2$, are the two components of the displacement vector. Application of Gauss's theorem yields

$$\alpha_{ij} = \frac{1}{V}\int_S u_j n_i dS, \tag{3.8}$$

where $\mathbf{n}$ is the unit vector normal to the boundary S. The average strain rate tensor is the symmetric part of $\bar{\alpha}_{ij}$:

$$\bar{\varepsilon}_{ij} = \frac{1}{2}(\bar{\alpha}_{ij} + \bar{\alpha}_{ij}). \tag{3.9}$$

The displacements in the pores are not uniquely defined. It is possible, as described by CUNDALL *et al.* [3], that the displacements assigned to the particles are real, whereas the displacements in the pores are chosen so that the displacement field is continuous throughout the domain. Another approach can be found in [11].

4. Test results

The history of deformation in one of the tests is shown in Fig. 8a. The uniformly compressed assembly of discs was subjected to shear. In the first stage this was done by an increase of boundary forces P_1 and P_2, step by step. Then P_1 increased and P_2 was kept constant. The dotted line and the dashed one are boundary displacements, u_1 and u_2, respectively, versus force P_1. The numbers on the dotted line indicate that the photo was taken at this stage of deformation. Figures 8b, c, d present the ellipses of geometric anisotropy and the polar diagrams which indicate the orientation of branch. There are the components of the fabric tensor $\bar{J}_{ij}$ and the parameters of geometrical anisotropy A_g and θ. The number at the center is the coordination number.

The orientation of the fabric of the sample shows the small initial anisotropy (AN1) which increases in the next stages (AN3, AN5). The direction of the predominant anisotropy is similar to the direction of P_1 (P_1 is the higher boundary force). It should be noted that a only part (about 90) of 1500 discs, making the neighbourhood of the brittle ring, was taken into account.

After crushing the grain (stage AN5), the geometrical anisotropy of the fabric has the characteristic of the cross-anisotropy. That cross-anisotropy, which can be seen more clearly after unloading stage AN6, suggests a manifestation of the discontinuity lines.

There are displacement vectores, in Fig. 9, which were found by comparison of photographs at various stages of the load. The displacement vectors are ten times greater than

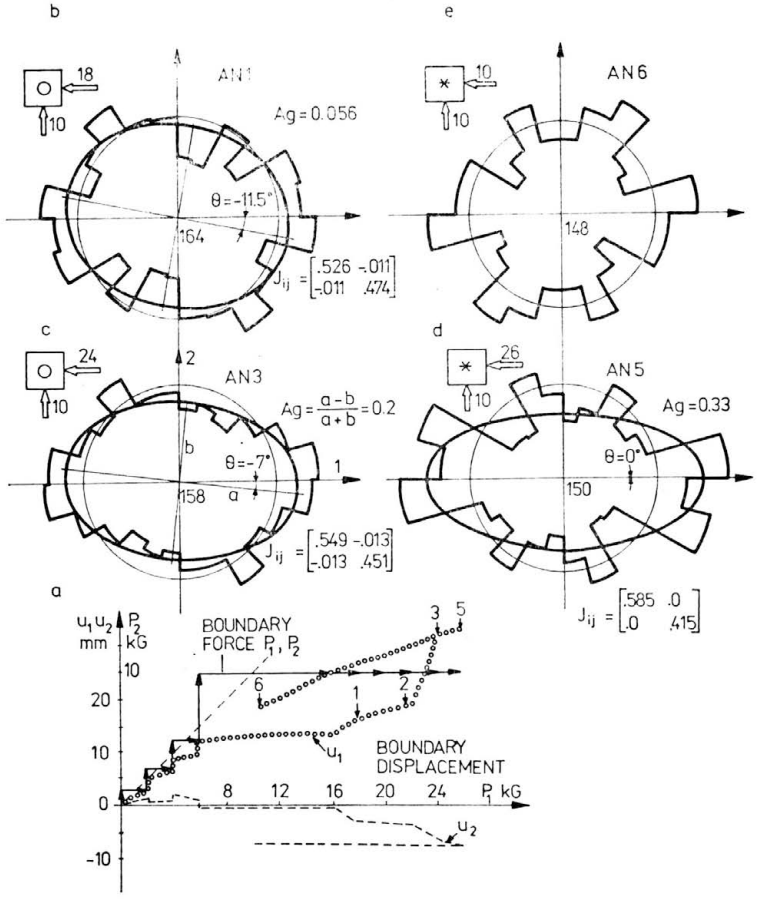

FIG. 8. History of deformation in shear test: a) forces and displacements at the boundary, b, c, d, e) distribution of normal contacts and geometrical anisotropy.

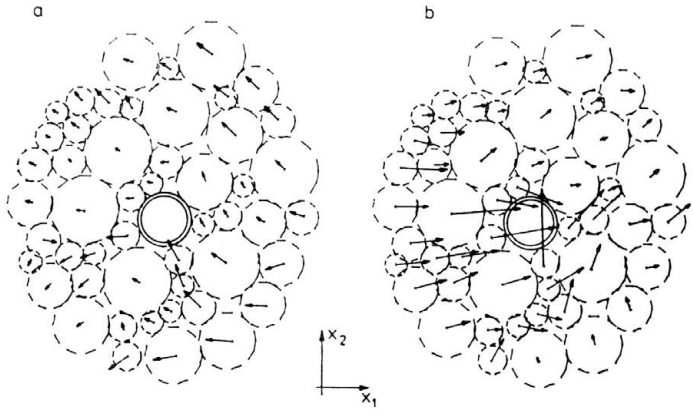

FIG. 9. Displacement vectors, a) before crushing, b) after crushing.

in reality. From these figures, using the averaging method described at Sect. 3.2, the strain rate tensor can be calculated.

Figure 10 shows the experimentally observed relation between the strain rate tensor components versus radius normalised to the radius of the crushed grain. The current radius r denotes the radius of the circle bounded over the averaging area. It is seen that the deformation before crushing is nearly uniform in the whole sample. As a result of

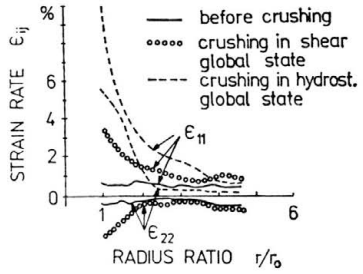

FIG. 10. Average strain rate tensor components calculated from experimentally obtained displacement vectors field.

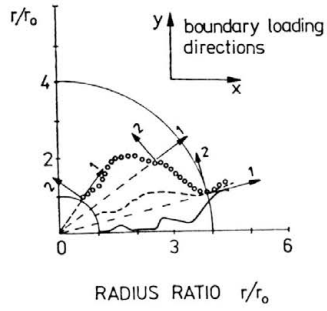

FIG. 11. Variation of principal directions of strain rate tensor.

crushing, large local deformation takes place. This nonuniform deformation vanishes with increase of r/r_0 ratio.

Figure 11 illustrates the variation of the principal directions of the strain rate tensor. Before crushing — solid line — the principal directions of the strain rate tensor are nearly constant, independently of the averaging area, and nearly coincide with load directions. After crushing — dotted line — the principal directions deviate strongly from the load directions, but for the domain of closely crushed grain only. For $r/r_0 = 4$ both principal directions, before and after crushing, coincide. It should be pointed out that the results presented in Figs. 8, 9, 10 and 11 are typical in all experiments.

5. Numerical experiments

An attempt was made to duplicate numerically the tests described above. It was possible to investigate the effect of crushing on the behaviour of the assembly, by repeating the experiments with the same geometry but different values of stiffness at contact between

the grains. The distinct element method, described by CUNDALL and STRACK [2], was used for numerical modelling. In this method the equilibrium of contact forces and displacements of a stressed assembly of discs are found through a series of calculations, tracing the movements of the individual particles. The calculations alternate between the application of Newton's second law to the discs and a force-displacement law at the contacts. Newton's second law gives the motion of a particle resulting from the forces acting on it. The force-displacement law is used to find contact forces from displacements. The time step chosen for calculation may be so small that during a single time step disturbances cannot propagate from any discs further than its immediate neighbours. It is this key feature of the distinct element method which makes it possible to follow the nonlinear interaction of a large number of discs without excessive computer memory requirements. The set of distinct element method programs, on the minicomputer SM4, similar to this one of the PDP 11 series, was constructed.

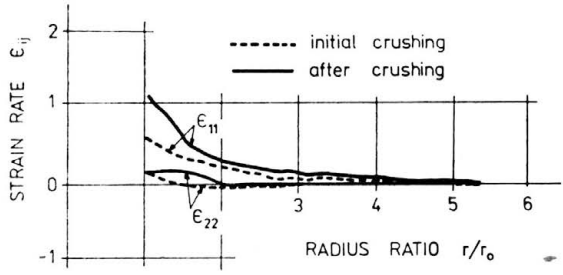

FIG. 12. Results of numerical experiment; average strain rate tensor components.

Figure 7a shows the assembly of discs chosen for numerical experiments. The structure of this assembly is similar but not the same, as in the physical experiment. The assembly of discs was loaded by means of two pairs of rigid beams which formed the boundaries. The crushing of a single grain was modelled by a rapidly changing radius of one grain in the central part of the sample. All the quantities used for the physical model description, as the strain rate, anisotropy or coordination number, in its average sense, were computed using the same methods as described earlier. Figure 12 shows a typical diagram of strain rate tensor components.

6. Damping effect

It follows from the presented results that the disturbance, caused by crushing of a grain, strongly depends on r/r_0. This relation can be called a damping effect. The curves taken from the experiments, normalised to r_0 and ε_0, which are illustrated in Fig. 13, correspond to the curve described by the following equation:

$$\varepsilon = \varepsilon_B + (\varepsilon_0 - \varepsilon_B)\exp\left[b - \left(\frac{r}{r_0} - 1\right)\right], \tag{6.1}$$

where b can be called a damping measure. It is interesting to note that the crushing effect, realised at various boundary conditions, with various configuration of discs, is characterised by, approximately, the same damping. The measured damping coefficient b is

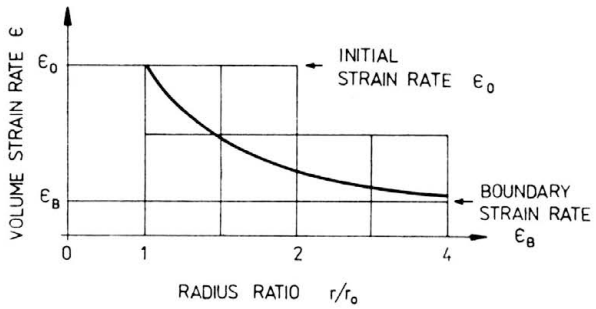

FIG. 13. Normalised damping curve.

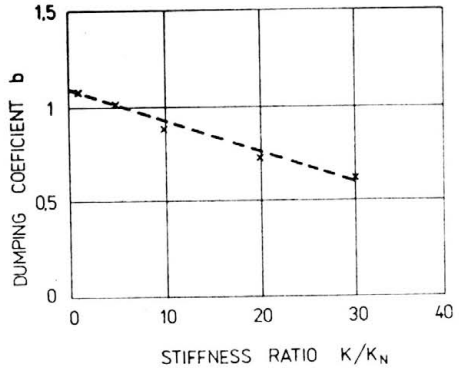

FIG. 14. Damping measure calculated from numerical experiments.

$$b_{px} = 1.01^{\pm 0.15} \text{ for plexiglass discs,}$$

$$b_{pu} = 1.57^{\pm 0.23} \text{ for poliuretane discs.}$$

It should be noted that the disturbance measure used above is a rather simple one. The measure of energy dissipation could be more precise but it requires the stress-strain relation which is not ready to be presented in this paper.

The results of the numerical experiment which make use of this damping measure can be described. In Fig. 14 the measure of damping b is plotted against the stiffness ratio k/k_n. That relation is nearly linear. The relative damping is inversely proportional to the relative stiffness, with factor a.

7. Conclusions

The conclusions may be summarized as follows:

1. The particle crushing effect does take place during the deformation of a cohesionless granular material.

2. The two-dimensional granular model of discs packed at random in the loading frame, with a single crushed grain, is useful to observe the crushing effect.

3. The disturbances caused by crushing of a single grain strongly depend on r/r_0. This damping effect can be described by formula (6.1).

4. The relative damping is inversely proportional to the relative stiffness.

References

1. J. BIAREZ, K. WIENDIECK, *La comparaison entre l'anisotropie mecanique et l'anisotropie de structure des milieux pulverulents*, C.R.Acad. Sci., **256**, 1217–1229, 1963.
2. P. A. CUNDALL, O. D. L. STRACK, *A discrete numerical model for granular assemblies*, Geotechnique, **29**, 47–65, 1979.
3. P. A. CUNDALL, A. DRESHER, O. D. STRACK, *Numerical experiments on granular assemblies; Measurements and observations*, IUTAM Conf., Delft 1982.
4. A. DRESHER, G. DE JOSSELYN DE JONG, *Photoelastic verification of a mechanical model for the flow of a granular material*, J. Mech. Phys. Solids, **20**, 337–351, 1972.
5. J. FEDA, *The effect of grain crushing on the peak angle of internal friction of sand*, Proc. 4th COSMFE, Budapest 1971.
6. M. R. HORNE, *The behaviour of an assembly of rotund, rigid, cohesionless particles* (I and II), Proc. Roy. Soc., A.**286**, 62–97, 1965.
7. M. R. HORNE, *The behaviour of an assembly of rotund, rigid, cohesionless particles* (III), Proc. Roy. Soc., A. **310**, 21–34, 1969.
8. G. MANDL, L. DE JONG, A. MALTHE, *Shear zones in granular material*, Rock Mechanics, **9**, 95–144, 1977.
9. R. J. MARSAL, *Mechanical properties of rockfill*, Embankment-Dam Engineering, Casagrande Vol., J. Wiley and Sons, New York 1973.
10. H. MATSUOKA, H. GEKA, *A stress-strain model for granular materials considering mechanism of fabric change*, Soils and Found., **23**, 83–97, 1983.
11. M. M. MECHRABADI, S. NEMAT-NASSER, *Stress, dilatancy and fabric in granular materials*, Mech. Materials, 2, 155–161, 1982.
12. N. MIURA, S. O-HARA, *Particle-crushing of a decomposed granite soil under shear stresses*, Soils and Found., **19**, 3, 1979.
13. N. MIURA, H. MURATA, N. YASUFUKU, *Stress-strain characteristic of sand in a particle crushing region*, Soils and Found., **24**, 1, 1984.
14. F. MOLENKAMP, *Decomposition of velocity gradient into interparticle slip and rolling*, Soils and Found., **24**, 1, 1984.
15. Z. MRÓZ, *Deformation and flows of granular materials*, Proc. IUTAM Congr., Toronto 1980.
16. H. ODA, *Fabric and their effects on the deformation behaviour of sand*, Dept. Fdn. Engng, Saitama University, Special Issue, 1–59.
17. M. ODA, J. KONISHI, S. NEMAT-NASSER, *Some experimentally based fundamental results on the mechanical behaviour of granular materials*, Geotechnique, **30**, 479–495, 1980.
18. M. ODA, S. NEMAT-NASSER, M. M. MECHRABADI, *A statistical study of fabric in a random assembly of spherical granules*, Int. J. Numer. Anal. Methods Geomech., **6**, 77–94, 1982.
19. M. ODA, S. NEMAT-NASSER, M. M. MECHRABADI, *A statistical study of fabric*, in: On Statistical Description of Stress and Fabric in Granular Materials, 6, 95–108, 1982.
20. M. ODA, J. KONISHI, S. NEMAT-NASSER, *Experimental micromechanical evaluation of strength of granular materials; effects of particle rolling*, Mech. Materials, 1, 269–283, 1982.
21. H. SATAKE, *Constitution of mechanics of granular materials through the graph theory*, Proc. US-Japan Seminar, Sendai, Japan 1982.
22. J. SUPEL, *Certain properties of granular media subjected to high pressure*, Engng Trans., 26, 101–113, 1978 [in Polish].
23. J. SUPEL, *The average number of contacts and its distribution for cohesionless granular materials* [in preparation].

POLISH ACADEMY OF SCIENCES
INSTITUTE OF FUNDAMENTAL TECHNOLOGICAL RESEARCH.

Received February 6, 1985.